Earth and Planetary Science Letters 502 (2018) 174–186

Contents lists available at ScienceDirect

Earth and Planetary Science Letters

www.elsevier.com/locate/epsl

Evidence of pervasive trans-tensional deformation in the northwestern Wharton Basin in the 2012 earthquakes rupture area

Nugroho Hananto [a], Asmoune Boudarine [b], Hélène Carton [b], Satish C. Singh [b,e,*], Praditya Avianto [a], Jérôme Dyment [b], Yanfang Qin [b], Dibakar Ghosal [c], Rina Zuraida [d], Paul E. Tapponnier [e], Christine Deplus [b], Kerry Sieh [e]

[a] Research Center for Oceanography, Indonesian Institute of Sciences, Jl Pasir Putih 1 Ancol Timur, Jakarta Utara 14430, Indonesia
[b] Equipe de Géosciences Marines, Institut de Physique du Globe de Paris (CNRS, Paris Diderot, Sorbonne Paris Cité), 1 rue Jussieu, 75238 Paris Cedex 05, France
[c] Indian Institute of Technology, Kanpur, India
[d] Marine Geological Institute, Jl DR. Junjunan 236, Bandung, Indonesia
[e] Earth Observatory of Singapore, Nanyang Technological University, N2-01A-XX, 50 Nanyang Avenue, Singapore 639798, Singapore

ARTICLE INFO

Article history:
Received 26 November 2017
Received in revised form 31 August 2018
Accepted 5 September 2018
Available online xxxx
Editor: J.-P. Avouac

Keywords:
the 2012 Indian Ocean earthquake
diffuse deformation
Wharton Basin
plate bending
shear zones
normal faults

ABSTRACT

The Wharton Basin in the Indian Ocean is one of the most extensively deforming ocean basins, as confirmed by the occurrence of several very large earthquakes starting from January 12, 2012 with Mw 7.2 followed by the great earthquakes of April 11, 2012 with Mw 8.6 and Mw 8.2. Although the Mw 7.2 and Mw 8.2 earthquakes seem to have ruptured the re-activated N–S striking fracture zones, the largest event (Mw 8.6) required the rupturing of several faults, oblique to each other, in a very complex manner. In order to understand the nature of deformation in these earthquakes rupture zones, we recently acquired 90 000 km^2 of bathymetry, 11 400 km of sub-bottom profiling, gravity and magnetic data covering the rupture areas of the 2012 earthquakes east of the Ninety-East Ridge, in the northwestern Wharton Basin. These new data reveal six N8°E striking re-activated fracture zones (F5b, F6a, f6b, F7a, F7b and F8), where the fracture zone F6a can be followed for over 400 km and seems to be most active. The epicenters of the Mw 8.6 and Mw 8.2 earthquakes lie on the fracture zones F6a and F7b, respectively. The newly observed fracture F5b in the east is short, and has an extensional basin at its southern tip. The fracture zone F8 defines the eastern boundary of the Ninety-East Ridge. The presence of en echelon faults and pull-apart basins indicate left-lateral motion along these fracture zones. In between these fracture zones, we observe pervasive 290° striking right-lateral shear zones at 4–8 km intervals; one of which has cut through a seamount that might have ruptured during the Mw 8.6 earthquake. We also observe another N20°E striking left-lateral shear zones in the vicinity of F7b and F8, which is coincident with the strike of one of the nodal planes of the Mw 8.6 focal mechanism. These N20°E striking shear zones are interpreted as R Riedel shears and the N290°E striking shear zones as R′ Riedel shears. These shear zones are formed by a series of N335°E striking en echelon normal faults. Our data also show the presence of N65°E striking thrust faults east of the Ninety-East Ridge, orthogonal to the regional principal direction of compression. Furthermore, extensive bending-related faulting is also observed close to the Sumatra trench with normal faults also striking at N335°E, similar to the normal faults that form the shear zones. Normal faults with a similar orientation are also present at the southern tip of F5b. We explain all these observations with a single coherent model of deformation in the Wharton Basin, where a dominant part of the regional NW–SE compressional stress is accommodated along the N8°E re-activated fracture zones, and the rest is distributed along shear zones, thrust and normal faults between these fracture zones. The thrust and normal faults are orthogonal to each other and define the direction of principal compressive and extensive stresses in the region whereas the two shear zone systems form a conjugate pair.

1. Introduction

The largest recorded intra-plate oceanic strike-slip earthquake of Mw 8.6 occurred on April 11, 2012 in the Wharton Basin with its epicenter about 120 km southwest of the Sunda trench. It was

* Corresponding author at: Equipe de Géosciences Marines, Institut de Physique du Globe de Paris (CNRS, Paris Diderot, Sorbonne Paris Cité), 1 rue Jussieu, 75238 Paris Cedex 05, France.
E-mail address: singh@ipgp.fr (S.C. Singh).

https://doi.org/10.1016/j.epsl.2018.09.007
0012-821X/

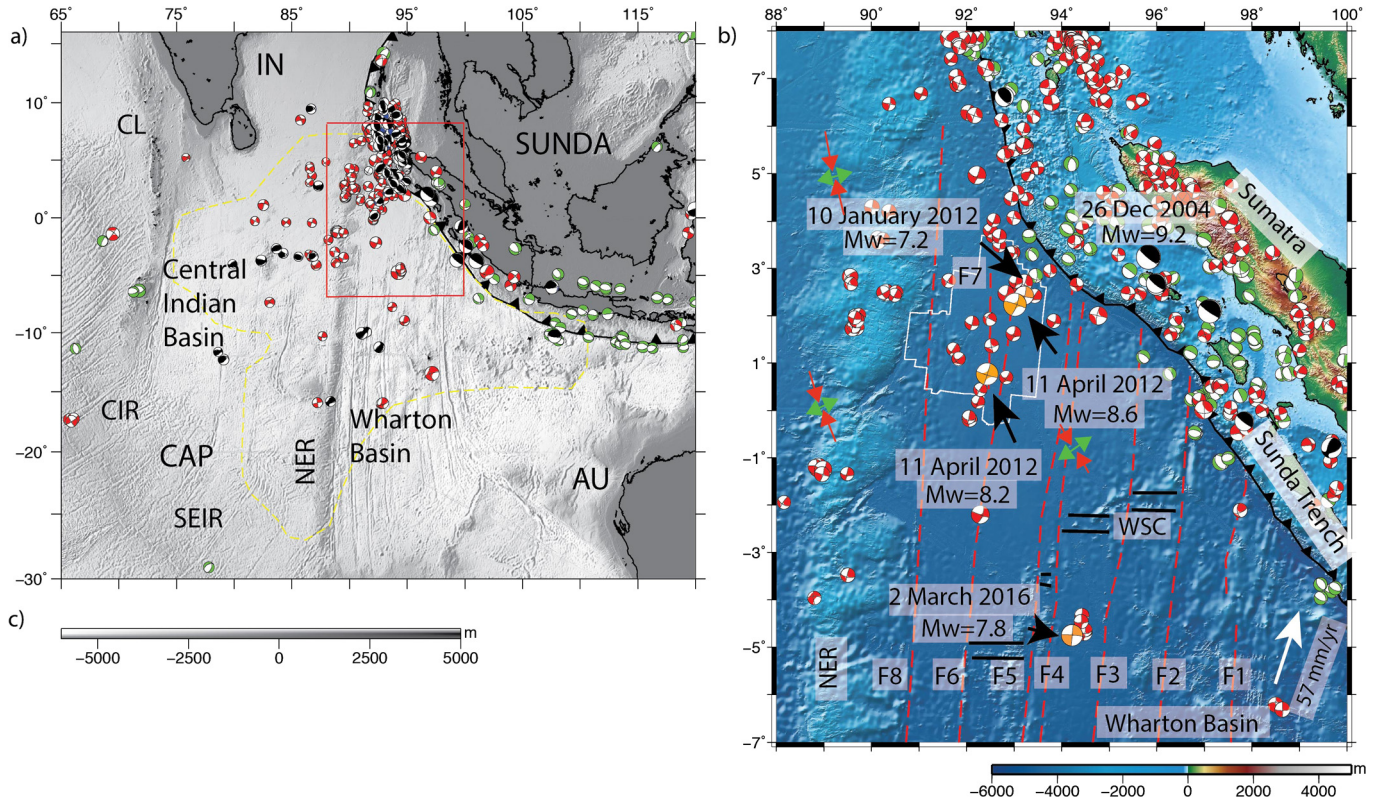

Fig. 1. (a) Regional tectonic setting of the composite Indo-Australian plate. Dashed yellow lines define the diffuse plate boundaries between IN (India), AU (Australia) and CAP (Capricorn) plates (after Royer and Gordon, 1997). Red box shows location of figure (b). CL = Chagos–Laccadive Ridge; CIR = Central Indian Ridge; SEIR = Southeast Indian Ridge; NER = Ninety-East Ridge. Seafloor topography is from ETOPO1 (Amante and Eakins, 2009). The beach balls indicate normal (green), thrust (black) and strike-slip (red) earthquakes. All the beach balls are plotted with their circle radii proportional to magnitude. (b) Oceanic plate structure in the Wharton Basin. Fracture zones (red dashed lines) and fossil Wharton Spreading Centre (double black line) are from Singh et al. (2011) identified from altimetry data. White arrows mark the convergence direction of the Indo-Australian Plate with respect to the Sunda Plate (Prawirodirdjo et al., 2000). Beach balls show historical seismicity recorded in the Wharton Basin since 2010. Focal mechanisms represent all magnitudes >5 Global CMT solutions (Ekström et al., 2012) from January 2010 to May 2017. Only Mw > 7.8 thrust earthquakes in the subduction zone are shown. The combined red–green arrows indicate the directions and the relative magnitudes of the principal deviatoric compression and tension components of stress (Gordon and Houseman, 2015). The three orange beach balls indicate the Mw 8.6 main shock and its Mw 8.2 aftershock, and Mw 7.2 foreshock. The 2nd March 2016 Mw 7.8 earthquake is also marked. The white line delimits the newly acquired bathymetric data shown in Fig. 3. (For interpretation of the colors in the figure(s), the reader is referred to the web version of this article.)

preceded by a foreshock of Mw = 7.2 on January 10, 2012 and followed by an aftershock of Mw = 8.2 two hours later (Duputel et al., 2012), along with hundreds of smaller aftershocks (Figs. 1, 2). It has been suggested that this earthquake occurred as a result of stress transfer on the incoming plate after the 2004 Mw 9.2 Sumatra–Andaman earthquake and the 2005 Mw 8.7 Nias earthquake (Delescluse et al., 2012).

This part of the Wharton Basin lies in a broad deformation zone within the composite Indo-Australian plate, extending from the Chagos–Laccadive ridge in the west to the Investigator Ridge in the east (Royer and Gordon, 1997) (Fig. 1a). Although this region is well known for distributed deformation within an oceanic plate (Gordon, 2000), many details about its seafloor morphology and tectonic activity are lacking, owing to its large extent and remote location. GPS and marine geophysical studies indicate that compressional faults and folds occur west of the Ninety-East Ridge (NER) in the Central Indian Basin south of India (Bull and Scrutton, 1990; Delescluse and Chamot-Rooke, 2007). In contrast, deformation is mainly accommodated by strike-slip faulting along re-activated N–S striking fracture zones in the Wharton Basin to the east of the NER (Deplus et al., 1998; Deplus, 2001) (Fig. 1b).

The occurrence of such a large earthquake with a high stress drop away from major plate boundaries came as a surprise (McGuire and Beroza, 2012). Although the foreshock and the main aftershock seem to have ruptured along re-activated fracture zones, the main event (Mw 8.6) appears to have ruptured several faults, oblique to one another, in a very complex manner (Hill et al., 2015; Wei et al., 2013; Ishii et al., 2013; Meng et al., 2012; Yue et al., 2012) (Fig. 2). This suggests that deformation in the northern Wharton Basin is distributed over a number of faults, but the exact geometry of this fault system and the identification of the main structures are still open questions. Most models based on seismological and geodetic studies agree that the Mw 8.6 main shock involved rupture on one NNE–SSW trending fault along with at least one WNW–ESE trending fault, with the seismic moment released dominantly during the NNE–SSW rupture. The limited existing bathymetry data show recent activity along these fracture zones (Deplus et al., 1998; Graindorge et al., 2008) but their strike is no more than 8°E (Carton et al., 2014; Singh et al., 2017). On the other hand, the GCMT solution for the main event shows one nodal plane striking 20°E, and none of the fault geometries associated with models of coseismic slip distribution align with the existing fracture zones (Fig. 2). Based on limited bathymetry (75 km by 100 km) and high-resolution seismic reflection data in the vicinity of the Mw 8.2 aftershock, Singh et al. (2017) found the existence of N294°E trending shear zones in addition to the N–S re-activated fracture zones, and suggested that these two fault systems form a conjugate pair of faults, accommodating the large-scale deformation observed in the Wharton Basin. However, the 2012 Mw 8.6 earthquake rupture extends over a very large area that is very poorly sampled by marine geophysical data, leading to major uncertainties regarding the exact location and geometry of faults activated during this earthquake.